WAVE PROPAGATION IN PLATES WITH PERIODIC ARRAY OF IMPERFECT ACOUSTIC BLACK HOLES

Bing Han[1], Hongli Ji[2] and Jinhao Qiu[3]

[1] Yudao Street 29, Nanjing 210016, China, State Key Laboratory of Mechanics and Control of Mechanical Structures, Nanjing University of Aeronautics and Astronautics, e-mail: zsdjxbing@126.com
[2] Yudao Street 29, Nanjing 210016, China, State Key Laboratory of Mechanics and Control of Mechanical Structures, Nanjing University of Aeronautics and Astronautics
Hung Hom, Kowloon 999077, Hong Kong, Department of Mechanical Engineering, Hong Kong Polytechnic University, e-mail: jihongli@nuaa.edu.cn
[3] Yudao Street 29, Nanjing 210016, China, State Key Laboratory of Mechanics and Control of Mechanical Structures, Nanjing University of Aeronautics and Astronautics, e-mail: qiu@nuaa.edu.cn

Keywords: Acoustic black hole, Periodic array, Dispersion relation, Finite element

ABSTRACT

Acoustic black hole (ABH) structure has been developed as an approach for attenuating structural vibration and manipulating wave propagation. Since energy concentration property of a single ABH structure is limited in its operating frequency range, it is needed to extend the low frequency performance of ABH systems for vibro-acoustic application and wave manipulating in low frequency. In this study, a thin plate with embedded periodic array of imperfect ABH structures is investigated for wave propagation study. Dispersion relations and displacement fields of eigenmodes calculated by the finite element method (FEM) change dramatically compared with the plate with periodic traditional ABH structures. Among these dispersion curves of the proposed structures, the flat band can easily be observed. The position of degenerate points and the symmetry of corresponding eigenmodes at the high symmetric point turns out to be different from these occurring in the case for periodic traditional ABH structures. Dispersion relations and eigenmodes of the proposed structures are effected by the key geometry parameters of ABH region. The thickness and the radius of the plateau in the middle, which is concerned primarily, have a great influence on dispersion relations. This study will aid in exploring the performance of wave propagation of the imperfect ABH systems below cut-off frequency.

1 INTRODUCTION

The Acoustic Black Hole (ABH) in thin-walled structures with a tailored power-law-profiled thickness, produces a reduction of the phase velocity of bending wave, and thus achieves energy concentration. Typical thickness profiles are with the form of $h(x)=\varepsilon x^m (m>2)$, such that the local phase velocity of the flexural waves reduces gradually and approaches zero theoretically when reaching the zero-thickness end of the tapered wage [1]. However, the ideal ABH is difficult to be manufactured, because truncations always exist at the edge or center of ABH. Typical two-dimensional ABH structures investigated in the literature usually contain a hole [2-4] or a circular plate of constant thickness located at the center of the indentation area [5]. Inevitably, these will affect the properties of ABH structure. Experimental measured frequency responses of two-dimensional ABHs, with a small central hole, were reported [2, 3] and these researches showed that the structural geometry parameters have influence on ABH phenomenon. In the absence of damping, the property of wave focalization of ABH structure can be developed as a method for manipulating the propagation of the flexural wave [6]. This property also can be utilized to control vibration and noise, which can be achieved by coating a small amount of damping materials at the ABH region to absorb focussed energy [7, 8].

For a single ABH structure, the wave must interact effectively with ABH structures to obtain effective wave focalization. The wavelength of the incoming wave should be at least of the same order or smaller than the diameter of the ABH structures for effective wave focalization, which indicates the existence of cut-off frequency. Therefore, the characteristic of wave focalization of ABH structure is

hampered when the vibrating frequency is below the cut-off one. It is necessary to extend and optimize the low-frequency-performance of ABH systems. The vibro-acoustic properties of a plate embedded with multiple two-dimensional traditional ABH structures was investigated and results show that the periodic array of ABH structure can improve its low frequency performance [4, 9]. The preliminary exploration of the propagation of wave in a plate with embedded periodic array of traditional ABH (PTABH) structures also was carried out [10].

In previous work, it has been proved that the energy focalization point in the imperfect ABH structure is different from that in traditional one [5]. Then it is much significant to analyse wave propagation characteristics in plate with embedded periodic array of imperfect ABH (PIABH) structures. The goal of this research is to investigate the eigenstate, which will aid in analysing the wave motion in PIABH structures. Therefore, we only focus on the study of dispersion relations and eigenmodes using finite element method (FEM) here. The results of PIABH case were compared with the PTABH one. The infection of key parameters of imperfect ABH was also analysed.

2 MODEL DESIGN AND SIMULATION

This section includes two parts: The first introduces the PIABH structure and the imperfect ABH indentation. A brief introduction of the 3D FEM used to calculate the dispersion relations was shown. Then the supercell plane wave expansion (PWE) method was also used to calculated dispersion relations. It can be found that the FEM is a more efficient method for calculating dispersion relations of infinite periodic ABH structures compared with PWE method.

2.1 PIABH structure design

The considered structure is a thin plate with embedded multiple imperfect ABH structures to form a two-dimensional square lattice with lattice spacing a (the lattice is 0.24 m in all numerical study), as show in Fig.1 (a). The z axis is along the plate thickness direction. Fig.1 (b) illustrates the schematic of the unit cell. The taper profile of the imperfect ABH structure can be seen in Fig.1 (c). The thickness of the plateau in the middle is equal to h_1 when $r \leqslant r_1$, and then the thickness of the tapered regions change gradually according to the function of $h(r)=a(r-r_1)^m+h_1 (r \leqslant r_1)$. The extreme case with $h_1=r_1=0$ and $m \geqslant 2$ corresponds to an ideal ABH structure. The thickness of ABH regions gradually change as following

$$h(r)=\begin{cases} h_1, & (r \le r_1) \\ a(r-r_1)^m + h_1, & (r_1 \le r \le r_2) \end{cases} \tag{1}$$

where h_1 is the constant thickness of the middle platform and the residual thickness of the tapered region. The material parameters are given in Table 1.

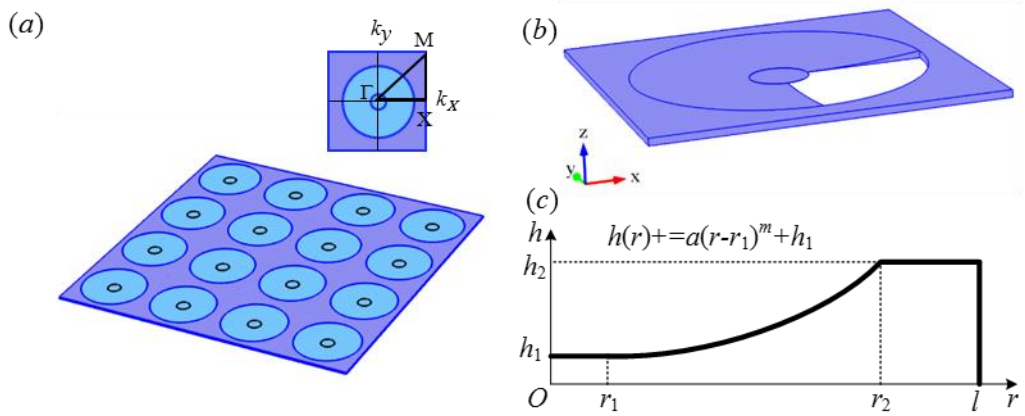

Figure 1: (a) Schematic of the thin plate with periodic imperfect ABH structures and the first Brillouin zone, (b) Supercell used for the FEM model, (c) Nonideally profiled ABH indentation.

Material	Density $\rho\left(kg/m^3\right)$	Young's modulus $E\left(10^{10}Pa\right)$	Poisson's ratio ν
Aluminum	2700	7×10^{10}	0.33

Table 1: Material parameters for structure

2.2 Finite element analysis

The wave solutions in the elastic plate with stress-free boundary condition can be determined completely by the elastic equation

$$\sum_{j=1}^{3}\left\{\frac{\partial}{\partial x_i}\left(\lambda\frac{\partial u_j}{\partial x_j}\right)+\frac{\partial}{\partial x_j}\left[\mu\left(\frac{\partial u_i}{\partial x_j}+\frac{\partial u_j}{\partial x_i}\right)\right]\right\}=\rho\frac{\partial^2 u_i}{\partial t^2},(i,j=1,2,3) \tag{2}$$

where the ρ is the density and u_j is the displacement component. In order to investigate the wave propagation characteristics of the proposed periodic plate-type structure, the dispersion relations and eigenmodes were calculated based on FEM and Bloch theory. For the unit cell shown in Fig.1 (b), stress-free boundary conditions were imposed naturally on the plate surfaces normal to z-direction, and periodic boundary conditions were applied to the interface between the nearest unit cells according to the Bloch-Floquet theorem

$$u_i(x_1+a,x_2+a,t)=u_i(x_1,x_2,t)e^{i\left(k_x a+k_y a\right)},(i=1,2,3) \tag{3}$$

where k_x and k_y are the components of Bloch wave vector limited in the irreducible first Brillouin zone. By sweeping the Bloch wave vector, the generated eigenvalue problem can be solved by FEM. COMSOL Multiphysics, a commercial software, was adopted to implement the FEM calculation procedures. Then the dispersion curves and mode shape can be obtained.

It is necessary to provide evidence supporting the FEM's ability to perform Bloch calculations. The dispersion relations of the plate with periodically embedded imperfect ABH structure using the supercell PWE method [10, 11] were compared with the results of using the FEM. The dispersion curves of the imperfect ABH cell for m = 2, r_1 =0.02 m, r_2 =0.1 m and h_1 = 0.0012 m are shown in Fig.2. The solid line represents the dispersion relations with finite element analysis. The dashed line correspond to the results obtained from supercell PWE method, where 169 reciprocal vectors in xy plane and 3 Fourier components in z direction were used. The results of the FEM match well with those of the supercell PWE method, indicating the capability of Bloch calculation using FEM.

It is worth noting that the structural characteristic of ABH results in the inhomogeneity of thickness of the thin plate, which has a significant effect on the convergence of the supercell PWE method. To illustrate this effect with quantitative analysis, the difference of the results given by the two methods is shown in Fig.3, when the thickness of the central circular plateau varies. The vertical axis δ represents the average error of the first m eigenfrequency calculated using the two methods. The value δ is given by

$$\delta=\frac{1}{m}\sum_{1}^{m}\frac{\left|f_m^{\mathrm{FEM}}-f_m^{\mathrm{PWE}}\right|}{f_m^{\mathrm{FEM}}}\times100\% \tag{4}$$

where f_m^{FEM} and f_m^{PWE} are the m-th eigenfrequency calculated by FEM and PWE methods (The number of the reciprocal vectors in xy plane and the Fourier components in z direction are 169 and 3.) respectively for a given Bloch wave vector. It can be observed that thinner thickness of the central circular plateau creates greater difference between the results of the two methods. The PWE method needs more reciprocal vectors in xy plane to obtain more accurate results and will costs more central processing unit (CPU) time. Therefore, the convergence of the PWE method is extremely slow, when the minimum structural thickness in the center is much thin. So the FEM was chosen as the more efficient method to calculate dispersion relations.

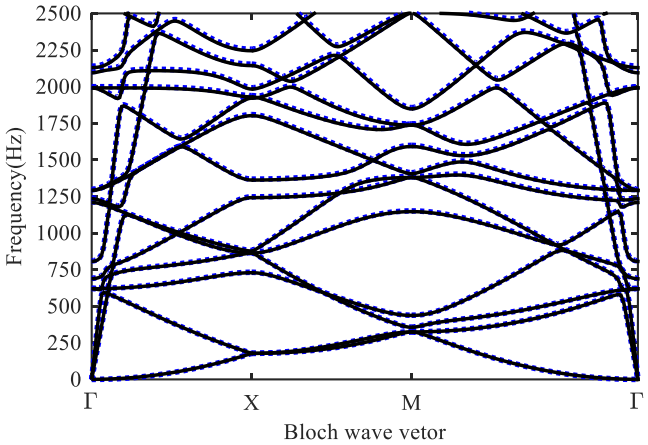

Figure 2: Dispersion curves of the supercell PWE method and the FEM. The solid and dotted lines present results of PWE and FEM, respectively.

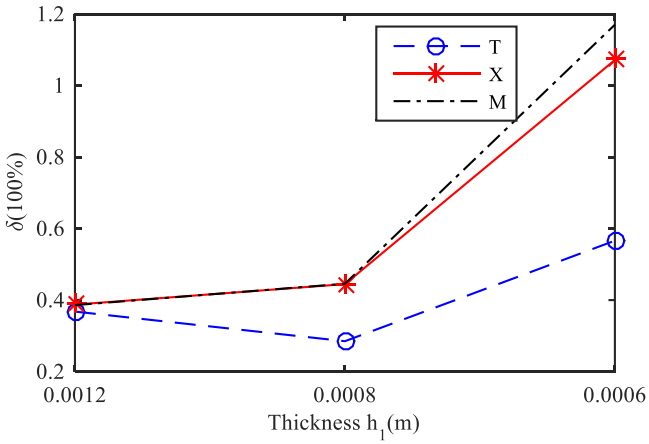

Figure 3: Calculation error between PWE and FEM methods with the variation of the thickness h_1 at symmetry points Γ, X, M.

3 NUMERICAL RESULTS AND DISCUSSION

Dispersion relations and eigenmodes of proposed PIABH structure were investigated in this section and the purpose of these simulations was to indicate that the performance of wave propagation in proposed PIABH structure is different from PTABH case. Then the influence of some defining parameters (i.e., thickness, power index, radius) on dispersion relations was also analyzed.

3.1 Dispersion relations and eigenmodes

In this section, the band structure of the proposed PIABH plate was calculated using the FEM, as shown in Fig.4 (a). The PIABH example consists of a 0.005-m-thick aluminum plate with tapers characterized by m = 2, r_1 =0.02 m, r_2 =0.1 m and h_1 = 0.0002m. For purpose of comparison, the plate embedded with periodic array of traditional ABH structure (Similar structure has been researched in Ref. [10]) was also considered, where the same radius r_2 and residual thickness h_1 in the center are chosen. The results of PTABH are presented in Fig.4 (b). For both cases, a narrow band gap can be found between the third dispersion relation and the second one along the XM direction in both PIABH and PTABH structures.

The significant difference is the flat band, meaning that the vibrational modes of the proposed structure is insensitive to the direction of incident wave at this frequency. The flat mode can be observed

in the PIABH case, while this only appears in the PTABH one with large parameter *m* [10]. Because of the presence of plateau, the band structures are disturbed and then more crossing-cover points are produced. It can be noted that there are more modes in unit frequency space for PIABH case.

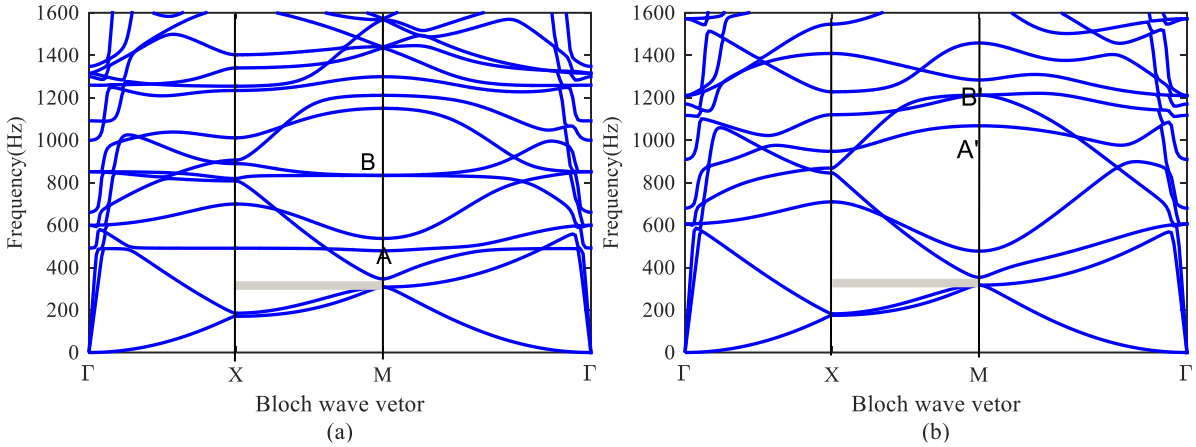

Figure 4: Dispersion relations along the irreducible part of the first Brillouin zone: (a) the PIABH case and (b) the PTABH case

The wave propagation in an ideal two-dimensional phononic crystal can be decoupled into the in-plane modes (*x*-*y* plane) and the out-of-plane modes [12]. However, the modes in periodic plate structure are classified into flexural (antisymmetric), longitudinal (symmetric), and transverse (horizontal shear) waves because the modes in the plate are coupled.

To investigate the influence of the imperfect ABH structure on wave modes in the dispersion relations, the polarization of specific modes was analyzed. The displacement field of the flat mode (A) observed in Fig.4 (a) is show in Fig.5 (a). It shows obvious local mode which can be characterized by monopole modal displacement field. For the PTABH case, the local mode shown in Fig.5 (b) is found at point A' labeled in Fig.4 (b). However, it can be seen that the corresponding branch is not a flat band.

Another significant difference is the change of the degenerate points called Dirac-like point [13, 14] at the high symmetric M point. The Dirac-like point are expected to produce some new wave propagation properties [15]. The displacement fields of the double degenerate B and B' at the high symmetry M point are shown in Figs. 6 (a)-(b) and (c)-(d) respectively. For the PIABH case, the displacement fields present a dipolar field pattern with a symmetry plane parallel to the *xz* plane or *zy* plane, while the dipolar field pattern of the PTABH case has a different symmetry plane. In other words, the wave fields in the plate with PIABH structure are different from that in PTABH one.

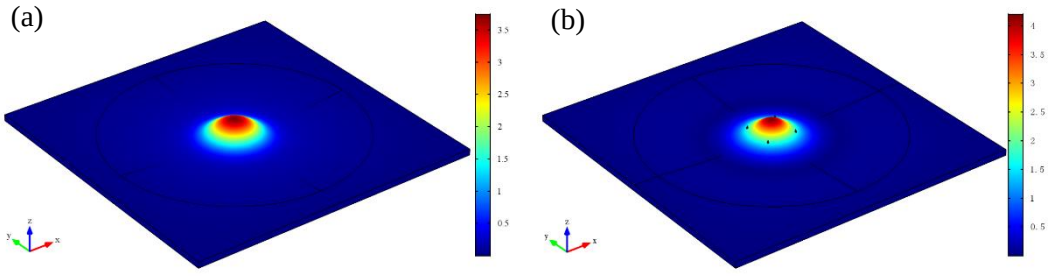

Figure 5: Eigenmode shape of the supercell at A labeled in Fig.4 (a) and A' in Fig.4 (b).

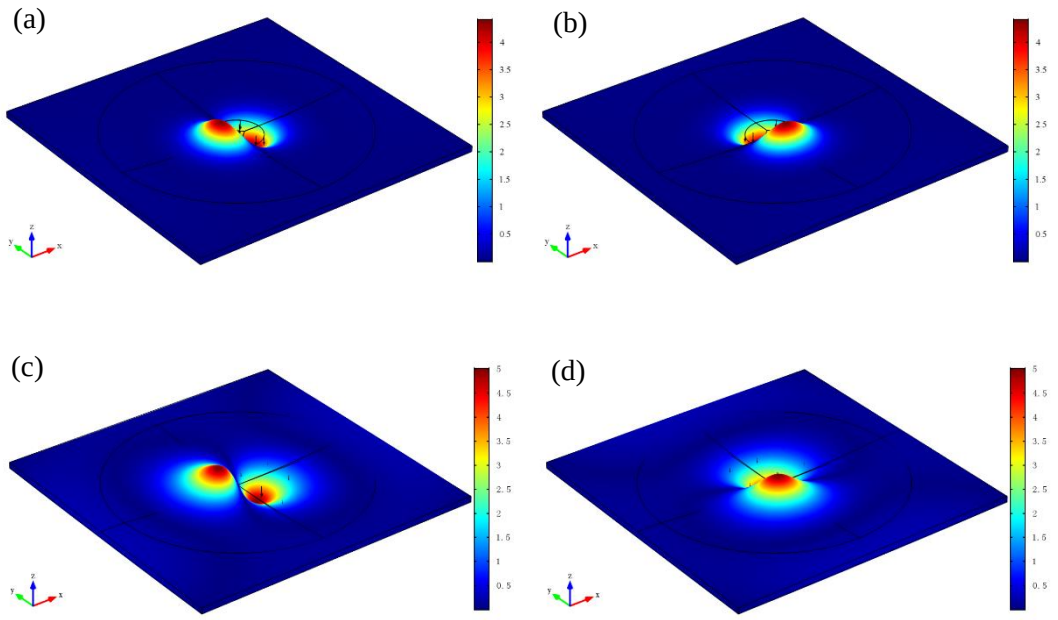

Figure 6: Eigenmode shape of the supercell at double degenerate point B labeled in Fig.4 (a) and B' in Fig.4 (b).

3.2 Influence of geometry parameters

It has been proved that the geometry parameters of the taper region have a great effect on the characteristics of single imperfect ABH in previous work [5]. Thereby, these parameters should also be taken into account to analyze the influence on dispersion relations and eigenmodes of the proposed structures.

To investigate the influence of the thickness of the plateau in the middle, the parameters of the tapered regions are taken as $m = 2$, $r_1 = 0.02$ m, $r_2 = 0.1$ m, where h_1 varies from $0.0002m$ to $0.0008m$. The radius of the ABH region r_2 is consistent in all numerical models. From Figs. 7 (a)-(c), it can be seen that the flat band is gradually disappear with the increase of the residual thickness of the tapered region. The flat mode is related to the local mode. The local vibration becomes more obvious with the decrease of the thickness h_1. The case with h_1=0.0008m shows little difference from that with h_1=0.0006m.

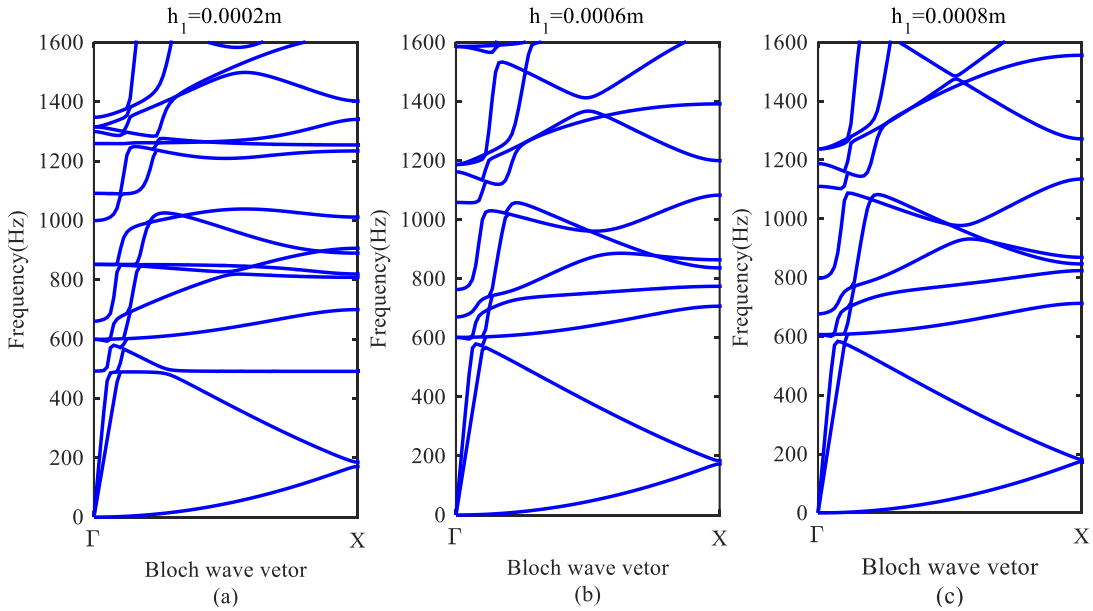

Figure 7: Dispersion relations for different thickness of the plateau: (a) h_1=0.0002m, (b) h_1=0.0006m, (c) h_1=0.0008m.

The other key design parameter is the power index *m*. The dispersion relations are shown in Figs. 8 (a)-(c) for m=1.5, 2, and 3 when r_1 =0.02 *m*. For all cases, the thickness of the plateau in the middle is constant and equal to 0.0002*m* by properly adjusting the coefficient *a*. There are more modes in unit frequency space when *m* is larger. Furthermore, of particular interest is that much more flat band can be seen when *m*=3.

Besides, the influence of radius r_1 of the circular plateau on dispersion relations is illustrated in Figs. 9 (a)-(c), where h_1=0.0002m and *m*=2. Overall, the flat band can easily come into being when radius is larger. The dispersion relations are gradually close to these of the PTABH case with the decrease of radius. That is because the local mode produced by the plateau in the middle generates less disturbance on the mode of entire structure.

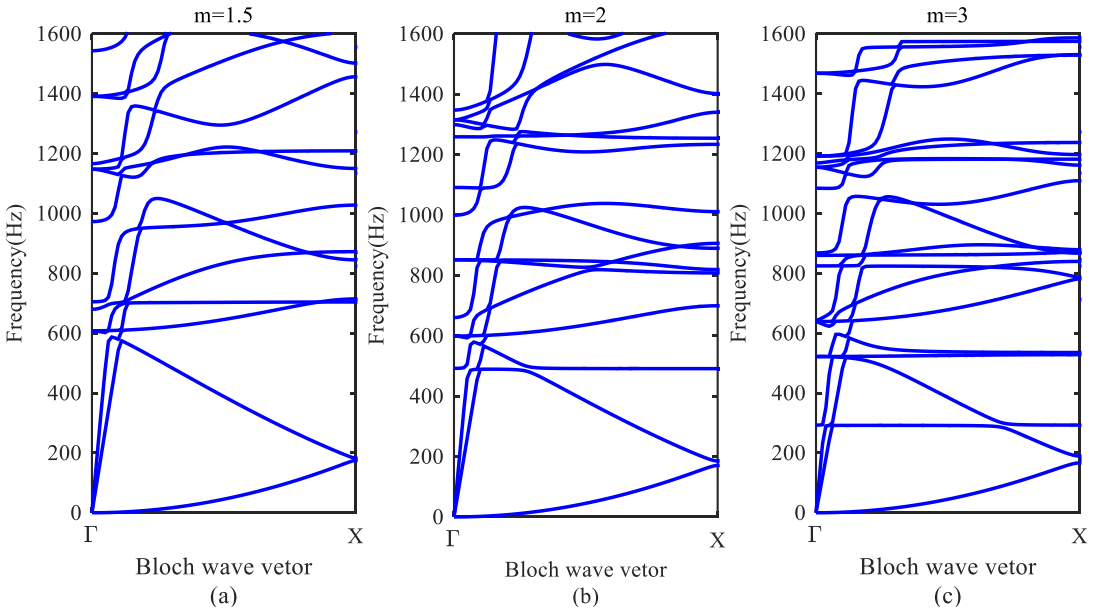

Figure 8: Dispersion relations for different power index: (a) *m*=1.5, (b) *m*=2, (c) *m*=3.

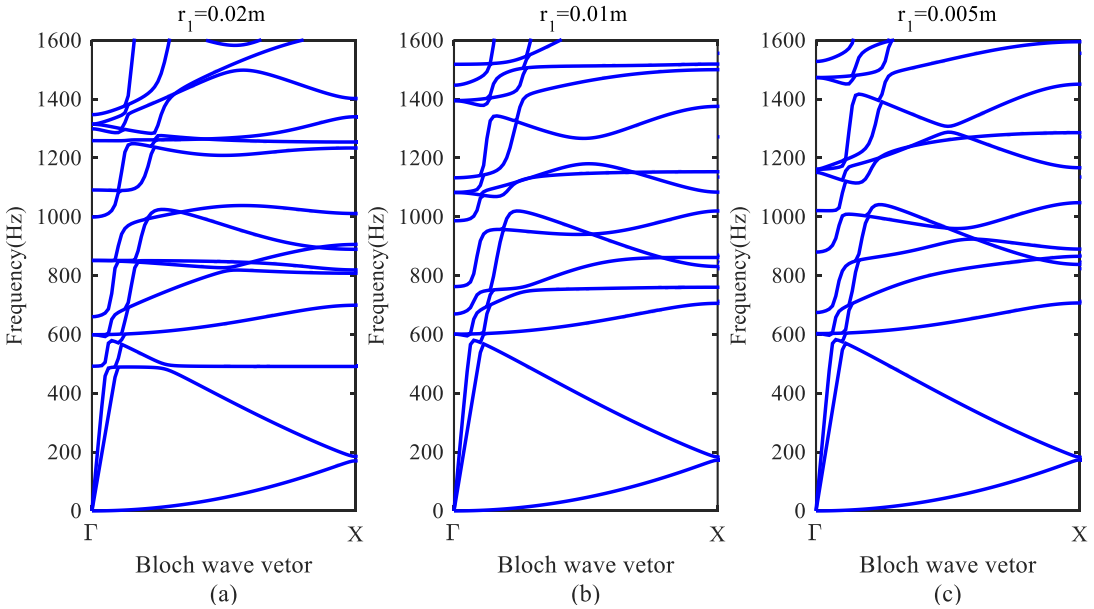

Figure 9: Dispersion relations for different radius of the plateau: (a) r_1 =0.02 *m*, (b) r_1 =0.01 *m*, (c) r_1 =0.005 *m*.

4 CONCLUSION

In this paper, dispersion relations of the plate with embedded periodic imperfect ABH structures were investigated. The dispersion curves of this structure are of interest, due to the existence of plateau in the middle of tapered region.

The proposed periodic structure has different dispersion relations compared with the similar periodic structure consisted of traditional ABH. The flat band can be seen in the PIABH case but not in PTABH case, when the power index *m* is equal to 2. By analyzing the eigenmodes of double degenerate points, we observed that the symmetry of the dipolar field pattern for the PIABH case differs from that in PTABH case. The influence of the key parameters of tapered profile on the dispersion curves was also analyzed. Results indicate that the thickness of circular plateau in the middle and the power index *m* have a greater impact on the dispersion relations than the radius of the plateau. However, these relations show little difference from the traditional case, when the thickness of the plateau is thicker and the radius is extremely small. This study is relevant to understanding the wave motion of the plate with periodic arrays of imperfect ABH structure.

Future work should be carried out to study the vibration properties and to achieve the goal of manipulating wave propagation in thin plate structures according to the specific dispersion relations investigated in this paper.

ACKNOWLEDGEMENTS

This research was supported by National Natural Science Foundation of China (No. 11532006), Research Grants Council of Hong Kong Special Administrative Region, China (PolyU 152009/15E), Fundamental Research Funds for the Central Universities (Nos. NE2015101 & NE2015001), Research Fund of State Key Laboratory of Mechanics and Control of Mechanical Structures (No. 0515Y02) and Aviation Science Foundation of China (20161552014).

REFERENCES

[1] M. A. Mironov, Propagation of a flexural wave in a plate whose thickness decreases smoothly to zero in a finite interval, *Soviet Physics: Acoustics,* **34**, 1988, pp. 318-319.

[2] E. P. Bowyer, D. J. O'Boy, V. V. Krylov, and F. Gautier, Experimental investigation of damping flexural vibrations in plates containing tapered indentations of power-law profile, *Applied Acoustics,* **74**, 2013, pp. 553-560.

[3] E. P. Bowyer and V. V. Krylov, Experimental investigation of damping flexural vibrations in glass fibre composite plates containing one- and two-dimensional acoustic black holes, *Composite Structures,* **107**, 2014, pp. 406-415.

[4] S. C. Conlon, J. B. Fahnline, and F. Semperlotti, Numerical analysis of the vibroacoustic properties of plates with embedded grids of acoustic black holes, *Journal of the Acoustical Society of America*, **137**, 2015, p. 447.

[5] H. Wei, J. Hongli, Q. Jinhao, and C. Li, Wave energy focalization in a plate with imperfect two-dimensional acoustic black hole indentation, *Journal of Vibration and Acoustics,* **138**, 2016, p. 061004.

[6] H. Zhu and F. Semperlotti, Improving the performance of structure-embedded acoustic lenses via gradient-index local inhomogeneities, *International Journal of Smart and Nano Materials*, **6**, 2015, pp. 1-13.

[7] V. V. Krylov and F. J. B. S. Tilman, Acoustic 'black holes' for flexural waves as effective vibration dampers, *Journal of Sound and Vibration*, **274**, 2004, pp. 605-619.

[8] V. V. Krylov and R. E. T. B. Winward, Experimental investigation of the acoustic black hole effect for flexural waves in tapered plates, *Journal of Sound and Vibration*, **300**, 2007, pp. 43-49.

[9] P. A. Feurtado and S. C. Conlon, An Experimental Investigation of Acoustic Black Hole Dynamics at Low, Mid, and High Frequencies, *Journal of Vibration & Acoustics,* 2016.

[10] H. Zhu and F. Semperlotti, Phononic Thin Plates with Embedded Acoustic Black Holes, *Physical Review B,* **91**, 2014, pp. 39-43.
[11] Z. Hou and B. M. Assouar, Modeling of Lamb wave propagation in plate with two-dimensional phononic crystal layer coated on uniform substrate using plane-wave-expansion method, *Physics Letters A*, **372**, 2008, pp. 2091-2097.
[12] J.-H. Sun and T.-T. Wu, Propagation of acoustic waves in phononic-crystal plates and waveguides using a finite-difference time-domain method, *Physical Review B,* **76**, 2007, p. 104304.
[13] F. Liu, Y. Lai, X. Huang, and C. T. Chan, Dirac cones at $\vec{k} = 0$ in phononic crystals, *Phys.rev.b,* **84**, 2011, p. 224113.
[14] F. Liu, X. Huang, and C. T. Chan, Dirac cones at $\vec{k} = 0$ in acoustic crystals and zero refractive index acoustic materials, *Applied Physics Letters,* **100**, 2012, pp. 1734-R.
[15] H.-F. Gao, X. Zhang, F.-G. Wu, Y.-W. Yao, and J. Li, Dirac-like point at the high symmetric M point in a square phononic crystal, *Solid State Communications,* **234-235**, 2016, pp. 35-39.